Toxicology and Applied Pharmacology 503 (2025) 117487

Contents lists available at ScienceDirect

Toxicology and Applied Pharmacology

journal homepage: www.elsevier.com/locate/taap

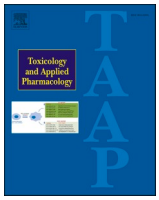

Systemic toxicity induced by topical application of the sulfonic acids, perfluorobutane sulfonic acid (PFBS) and perfluoropentane sulfonic acid (PFPeS), in a murine model

Madison P. Cooper [a,b,*,1], Lisa M. Weatherly [a,1], Ewa Lukomska [a], Laurel G. Jackson [a], Stacey E. Anderson [a]

[a] Allergy and Clinical Immunology Branch, Health Effects Laboratory Division, National Institute for Occupational Safety and Health, Morgantown, WV, United States of America
[b] Department of Microbiology, Immunology, and Cell Biology, West Virginia University, Morgantown, WV, USA

ARTICLE INFO

Editor: Lawrence Lash

Keywords:
Perfluorobutane sulfonic acid (PFBS)
Perfluoropentane sulfonic acid (PFPeS)
Toxicity
Immune
Dermal
Liver Damage

ABSTRACT

Per- and polyfluoroalkyl substances (PFAS) are a large group of synthetic surfactants incorporated into products for their chemical and physical properties. Studies have associated PFAS with adverse health effects. Although there is a high potential for dermal exposure, toxicity studies related to this route of exposure are lacking. The present study evaluated the systemic toxicity following a sub-chronic 28-day dermal exposure to perfluorobutane sulfonic acid (PFBS) (1.25–5 %) or perfluoropentane sulfonic acid (PFPeS) (1.25–5 %) in a murine model. Elevated levels of both PFAS were detected in the serum and urine, suggesting that absorption occurs through the skin. Additionally, both PFAS induced significantly increased relative liver weight, altered serum chemistries, altered skin and liver histopathology, and significantly decreased relative spleen weight (PFPeS only). Gene expression changes were observed in the liver and skin for genes involved in fatty acid metabolism, inflammation, and skin integrity. In general, the PFPeS-induced changes in the endpoints examined were observed more frequently compared to PFBS, supporting the concept that longer-chain PFAS are more toxic. These findings support PFAS absorption through the skin, leading to liver damage and systemic toxicity.

1. Introduction

Per- and polyfluoroalkyl substances (PFAS) are synthetic chemicals originally introduced in the 1940s with extensive applications for consumer and industrial products because of their unique and favorable chemical and physical properties, including liquid repellency, thermal stability, and friction-reduction. For this reason, PFAS are used in carpet, furniture, clothing, cookware, cosmetics, firefighting foam, lubricants, etchants, and surfactants (Gluge et al., 2020). There are thousands of PFAS, and more are constantly in production. During the manufacture, distribution, and use of products or processes containing PFAS, humans may be exposed to intentionally added PFAS, their byproducts, or impurities containing PFAS.

Due to the health effects associated with PFAS exposure, industry and government actions banned production of the legacy PFAS perfluorooctanoic acid (PFOA) and perfluorooctane sulfate (PFOS); however, owing to their environmental persistence and long half-lives, exposure to these substances is still a concern. Because of their desirable properties, safer proposed replacement PFAS, consisting of shorter carbon-chain formulas, have rapidly emerged. In general, these replacement PFAS have been promoted as safer alternatives due in large part to shorter half-lives in animal models (Wang et al., 2013). However, research continues to suggest that exposure to these emerging compounds may result in similar adverse health outcomes to PFOA and PFOS (Gomis et al., 2018; Weatherly et al., 2024a, 2024b; Weatherly et al., 2021; Weatherly et al., 2023). Much of what we know about PFAS-associated health effects in humans was generated from epidemiological studies on occupationally exposed individuals or from accidental releases near chemical manufacturing (Alexander et al., 2024; Darrow et al., 2016), but research is bringing more evidence for health implications to light (Panieri et al., 2022). Results from these studies suggest associations between PFAS exposure and certain types of cancers

* Corresponding author at: Department of Microbiology, Immunology, and Cell Biology, West Virginia University, Morgantown, WV 26505, USA.
E-mail address: mpc0011@mix.wvu.edu (M.P. Cooper).
[1] Co and equal first authors.

https://doi.org/10.1016/j.taap.2025.117487
Received 22 May 2025; Received in revised form 23 July 2025; Accepted 23 July 2025
Available online 24 July 2025

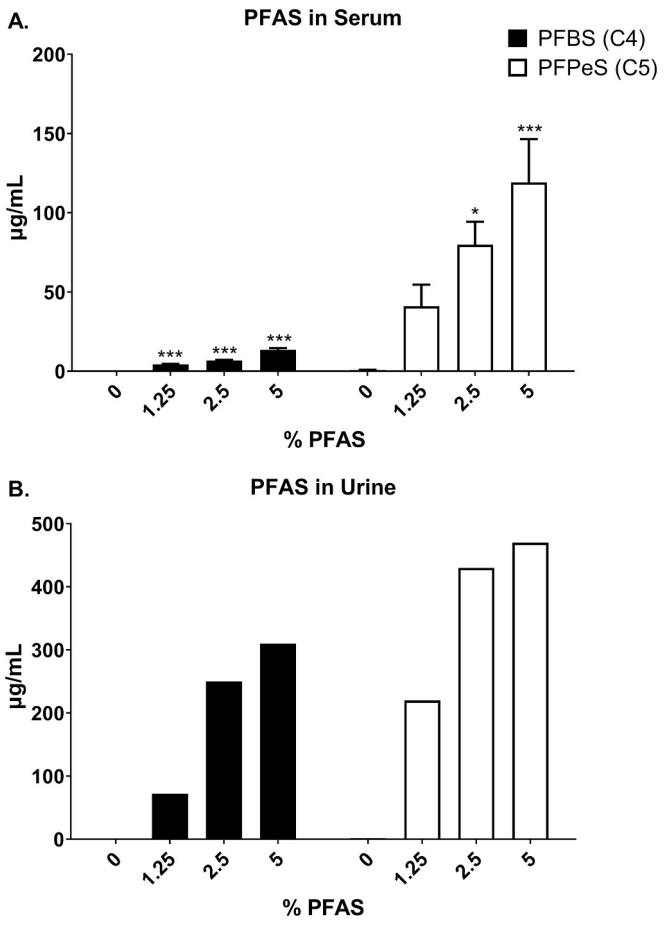

Fig. 1. Increases in PFBS and PFPeS concentration in serum and urine after dermal exposure. Analysis of changes in the concentration of PFBS and PFPeS in serum (A) and urine samples (B) following 28 days of skin exposure. Each serum concentration represents the mean (± SE) of 4–5 mice/group. Urine concentrations are 5 pooled samples per group. For the serum data, statistical significance, relative to 0 % vehicle control, was determined by one-way ANOVA followed by Dunnett's post-test, indicated as $*p < 0.05$, $***p < 0.001$.

(testicular and kidney), increased cholesterol levels, altered thyroid function, and reproductive effects (Fenton et al., 2021; Steenland et al., 2020). Additionally, the National Toxicology Program (NTP) concluded that both PFOA and PFOS are presumed immune hazards to humans based on evidence from animal and human studies (NTP, 2019). Furthermore, PFOA was identified as a carcinogen (Group 1) based on sufficient evidence generated from experimental animal and mechanistic human studies (Zahm et al., 2024).

PFAS legislation is appearing across federal and state governments, the National Academy of Sciences convened a workshop concerning federal agency PFAS research gaps, and academic, community, and private sector organizations are participating in innovative PFAS work. Numerous federal and regulatory agency working groups have determined specific research needs and gaps related to PFAS exposure, and there are ongoing robust public engagement efforts between federal agencies, states, local communities, utilities, industry, and the public to meet these needs. One clear knowledge gap is the adverse impact of PFAS on the health of workers, a topic heavily reliant on understanding dermal exposures (Fenton et al., 2021). This gap is reflected by the federal PFAS strategic planning committee's statements that additional pathways and routes of exposure to PFAS from indoor and outdoor environments need to be investigated (NSTC PFAS Strategy Team, 2023, 2024). This committee and others also emphasize the need to investigate potential risks from dermal PFAS exposure to help inform risk management (ITRC, 2023). Although dermal exposure data for PFAS is increasing, it is still limited (NSTC PFAS Strategy Team, 2023; Ragnarsdóttir et al., 2022).

The potential for worker dermal exposure to PFAS is high, both during the manufacturing process and in post-manufacturing workplace encounters with commercial products such as firefighting foams and carpet or fabric protectants (Gaines and Nylander-French, 2023; Lucas et al., 2023). Additionally, there is also concern for population exposure through the skin from groundwater (McMahon et al., 2022; Tokranov et al., 2024). Despite the potential for skin exposure, most research has focused on the toxic effects of oral PFAS exposure. However, previous data published in our laboratory and others suggest PFAS are absorbed through the skin of animals and 3D tissue models (Franko et al., 2012; Ragnarsdóttir et al., 2024). Similar to what has been described following oral exposure, PFOA is immunosuppressive following dermal exposure when evaluated in a murine model (Fairley et al., 2007; Shane et al., 2020). Since the potential for skin exposure to long-chain PFAS is still a concern due to environmental persistence, and short-chain PFAS are increasingly used both by consumers and occupationally (Gaines and Nylander-French, 2023), it is important to further understand the potential for penetration and the health risks from skin exposure to PFAS.

Therefore, the studies described in this manuscript are the completion of an effort to evaluate and compare the dermal penetration and toxicity of a series of occupationally relevant PFAS following repeat dermal exposure, including short-chain and long-chain (C4 to C8) PFAS with sulfonic acid or carboxylic acid functional groups (Weatherly et al., 2024a, 2024b; Weatherly et al., 2021; Weatherly et al., 2023). The PFAS compounds of interest were selected for the studies based on known and suspected worker exposures and include, perfluorobutanesulfonate (PFBS), perfluoropentanesulfonate (PFPeS), perflurorohexanesulfonate (PFHxS), perfluoroheptanesulfonate (PFHpS), perfluorooctanesulfonate (PFOS) (sulfonic acids C4–8), perfluorobutyric acid (PFBA), perfluoropentanoic acid (PFPeA), perfluorohexanoic acid (PFHxA), perfluoroheptanoic acid (PFHpA), and perfluorooctanoic acid (PFOA) (carboxylic acids C4–8) (Andres et al., 2024; Trowbridge et al., 2020; Wu et al., 2019). This manuscript reports the data and findings for PFBS and PFBA. The described studies provide data necessary to begin to address gaps in PFAS exposure assessments and our understanding of the hazards posed by PFAS exposure.

2. Materials and methods

2.1. Animals

Female $B_6C_3F_1$ mice were used in these studies as they are the National Toxicology Program's preferred strain for evaluating general toxicity and have been used previously to investigate PFAS immunotoxicity (Shane et al., 2020; Weatherly et al., 2021; Weatherly et al., 2023). All mice were purchased from Jackson Laboratory (Bar Harbor, ME) at 7–8 weeks of age. Upon arrival, the animals were allowed to acclimate for a minimum of 5 days. All animals were randomly assigned to treatment groups, weighed, and individually identified via tail marking using a permanent marker. Dose groups were identified by cage cards. Both the dosing group as well as the animal numbers were identified on each cage. The animals were housed 5 mice/cage in ventilated plastic shoe box cages with hardwood chip bedding, modified NIH-31 6 % irradiated rodent diet (Harlan Teklad – item #7913), and sterile tap water from water bottles *ad libitum*. The temperature in the animal facility was maintained between 65 and 78 °F and the relative humidity between 30 and 70 %; a light/dark cycle was maintained at 12-h intervals. All animal experiments were performed in an AAALAC International-accredited National Institute for Occupational Safety and Health (NIOSH) animal facility in accordance with an animal protocol approved by the CDC-Morgantown Institutional Animal Care and Use Committee. This activity was reviewed by CDC, deemed research not involving human subjects, and was conducted consistent with applicable

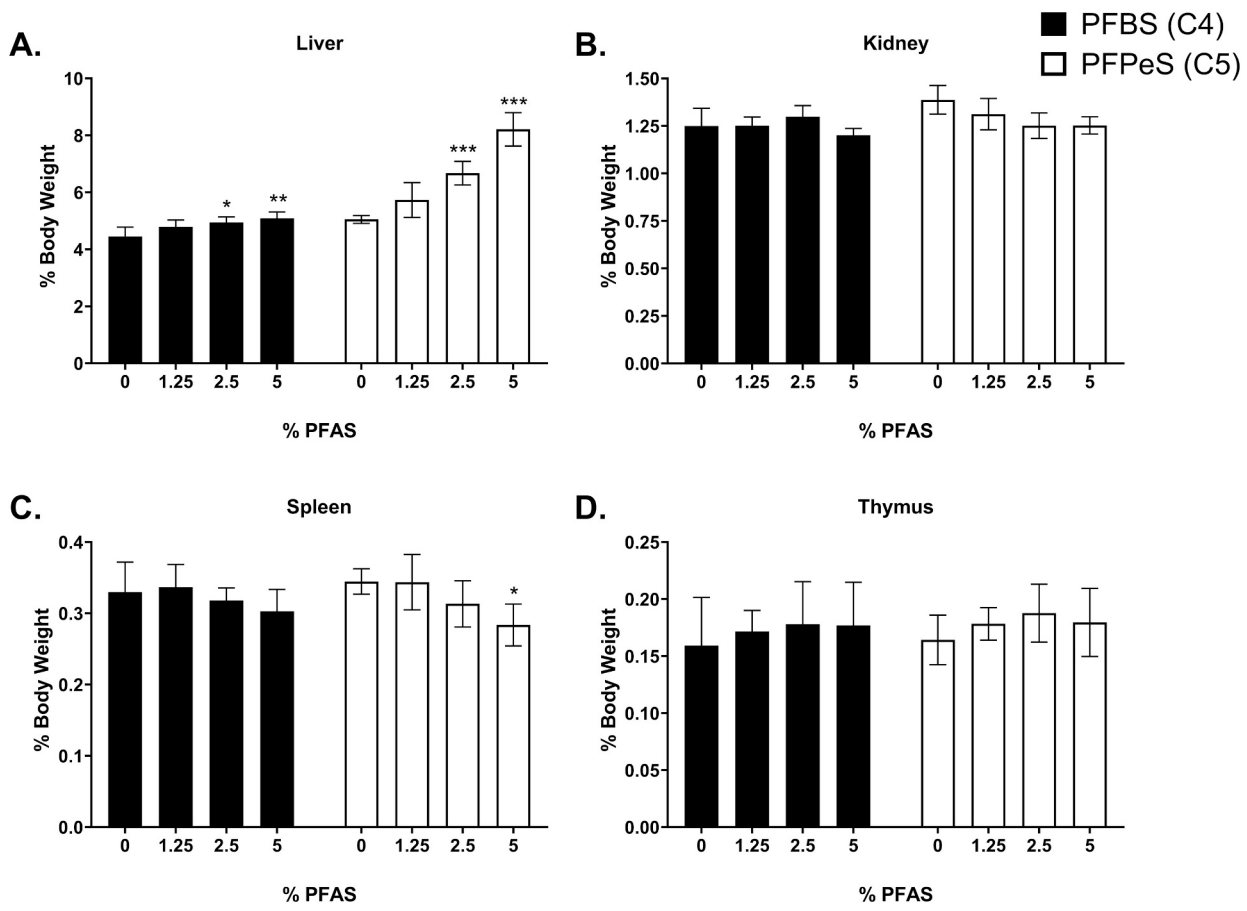

Fig. 2. Changes in relative organ weights after dermal exposure to PFBS or PFPeS. Analysis of changes in (A) liver, (B) kidney, (C) spleen, and (D) thymus weights following 28 days of exposure. Organ weight data is displayed as % body weight. Each concentration represents the mean (± SE) of 5 mice/group. Statistical significance, relative to 0 % control, was determined by one-way ANOVA followed by Dunnett's post-test indicated as *$p < 0.05$, ***$p < 0.001$.

federal law and CDC policy.

2.2. Test articles and chemicals

Acetone [CAS #67–64-1] and perfluorobutane sulfonic acid (97 %, PFBS) [CAS #375–73-5] were purchased from Sigma-Aldrich. Perfluoropentane sulfonic acid (95 %, PFPeS) [CAS #2706-91-4] was purchased from SynQuest Laboratories.

2.3. PFAS exposures

To evaluate systemic toxicity, $B_6C_3F_1$ mice (5/group) were topically treated on the dorsal surface of each ear (25 μL/ear) with vehicle (acetone), PFBS (C4), or PFPeS (C5) concentrations (1.25, 2.5, 5 % *v*/v) once a day for 28 consecutive days. This yielded an approximate topical daily dose of 226, 113, or 57 mg/kg body weight of PFBS(C4) and 225, 113, and 56 mg/kg body weight of PFPeS. Five mice per group have previously been shown to be sufficient to obtain statistical significance (Weatherly et al., 2024a, 2024b; Weatherly et al., 2021; Weatherly et al., 2023). These studies were conducted for the purpose of hazard identification, and the concentrations of PFBS and PFPeS were selected based on an initial 7-day range finding study and previous skin exposure studies conducted with various PFAS (Weatherly et al., 2024a, 2024b; Weatherly et al., 2021, Weatherly et al., 2023). Body weights were measured weekly and before exposure to ensure no overt toxicity was occurring. Animals were euthanized by CO_2 asphyxiation approximately 24 h after the last exposure.

2.4. Tissue processing

Following euthanasia, animals were weighed and examined for gross pathology. The liver, spleen, kidneys, and thymus were removed, cleaned of connective tissue, and weighed. Left and right auricular draining lymph nodes (dLNs; draining the site of chemical application), one half of the spleen, and one ear pinna were collected and placed in 4 mL RPMI for immune phenotyping as previously described (Weatherly et al., 2021). Half of one ear pinna and a small lobe of the liver (caudate) were placed in 0.5 ml of RNAlater for subsequent gene expression analysis (see below). The remainder of the liver, spleen, ear pinna (1/2), and one kidney (right) were collected in 10 % formalin for histopathology analysis.

2.5. Serum chemistries

Blood samples were collected following euthanasia via cardiac puncture, transferred to serum separation tubes, and separated by centrifugation. The serum was frozen at −20 °C for subsequent analysis. Selected serum chemistries were evaluated using a Catalyst DX Chemistry Analyzer (IDEXX Laboratories, Inc.; Westbrook, ME). Endpoints analyzed included: alkaline phosphatase (ALKP), urea nitrogen (BUN), glucose (GLU), alanine aminotransferase (ALT), and cholesterol (CHOL).

2.6. Analytical PFAS detection

Serum and urine samples were collected and analyzed for PFBS or PFPeS by Vista Analytical Laboratory, following Vista's standard operating procedures (Vista Analytical Laboratory, El Dorado Hills, CA) of

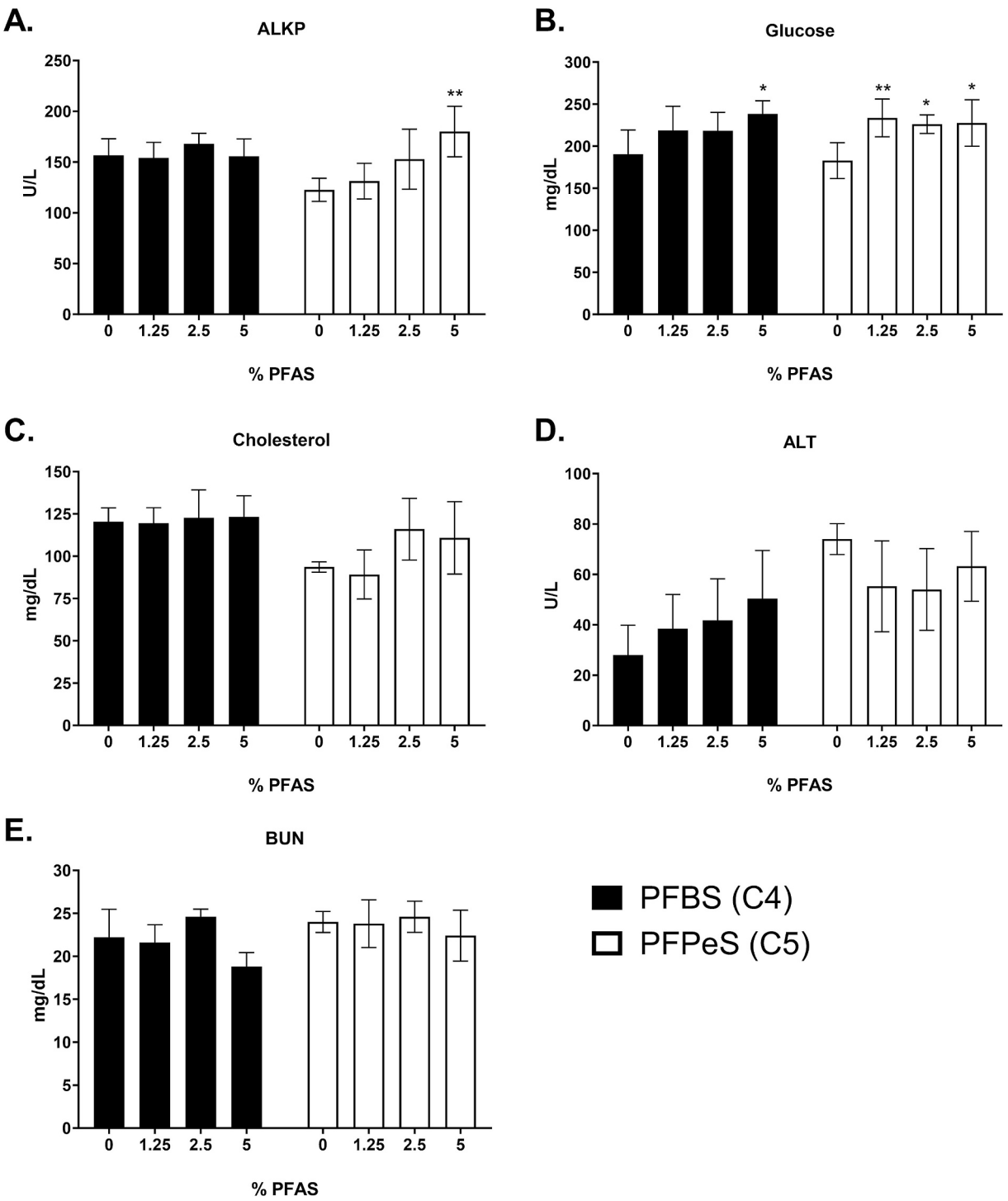

Fig. 3. Changes in serum chemistry after dermal exposure to PFBS or PFPeS. Analysis of changes in (A) alkaline phosphatase (ALKP), (B) glucose (C), cholesterol, (D) alanine aminotransferase (ALT), and (E) urea nitrogen (BUN) following 28 days of exposure. Each concentration represents the mean (± SE) of 4–5 mice/group. Statistical significance, relative to 0 % vehicle control, was determined by one-way ANOVA followed by Dunnett's post-test, indicated as *p < 0.05, **$p < 0.01$.

solid phase extraction and liquid chromatography/tandem mass spectrometry (LC/MS/MS) using BEH C18 columns as previously described (Shoemaker et al., 2008). Vista Analytical follows EPA method 537. An aliquot of serum was collected (as described above) from each animal following euthanasia. To have sufficient volume for analysis, voided urine was pooled following euthanasia and stored at −20 °C. The initial calibration and continuing calibration verifications met the acceptance criteria as previously described (Shoemaker et al., 2008). No analytes were detected in the method blank above the reporting limit (200 ng/mL). The labeled standard recoveries for all quality controls and samples were within the acceptance criteria as previously described (Shoemaker et al., 2008). PFBS concentration was set to zero in samples where PFBS was reported as 'Not Detected.'

2.7. Flow cytometry

Flow cytometry was conducted as previously described (Weatherly et al., 2021). For staining, single cell suspensions were resuspended in

Table 1
Incidence and degree of organ injury following dermal exposure to PFBS or PFPeS in mice.

	28 days							
	PFBS (C4) (v/v)				PFPeS (C5) (v/v)			
Parameter	0 %	1.25 %	2.5 %	5 %	0 %	1.25 %	2.5 %	5 %
Liver								
Hypertrophy, hepatocyte								
Minimal	0	0	0	5	0	3	0	0
Mild	0	0	0	0	0	1	5	0
Moderate	0	0	0	0	0	0	0	5
Necrosis								
Minimal	0	0	0	0	0	0	3	2
Ear/Skin								
Epidermis hyperplasia								
Minimal	0	1	3	5	0	0	0	5
Mixed cell inflammation, dermis								
Minimal	0	0	1	2	0	0	0	3

staining buffer containing anti-mouse CD16/32 antibody (Fc Block; BD Biosciences), then incubated with a cocktail of fluorochrome-conjugated antibodies specific for mouse cell surface antigens. For dLN and spleen cells: B220-V500 (RA3-6B2), CD11b-PerCP-Cy5.5 (M1/70), CD8-PE-CF594 (53–6.7), Siglec-F-PE (E50–2440), Ly6G-FITC (1A8) (BD Biosciences), CD11c-eFluor 450 (N418), CD86-APC (GL1) (eBioscience), CD45-Superbright 780 (30-F11), F4/80-PE-Cy7 (BM8), MHCII-APC-eF780 (M5/114.15.2) (Invitrogen), CD4-BV711 (RM4–5), Ly6C-AF700 (HK1.4) (BioLegend). For ear pinna cells: CD4-BV711 (RM4–5), NKp46-BV605 (29A1.4) (BioLegend), CD8-PE-CF594 (53–6.7), CD3-V500 (500A2), Ly6G-FITC (1A8), CD11b-PerCP-Cy5.5 (M1/70), CD11c-AF700 (HL3), Siglec-F-PE (E50–2440) (BD Biosciences), F4/80-PE-Cy7 (BM8), MHCII-APC-eF780 (M5/114.15.2), CD45-Superbright 780 (30-F11), FcεRI-APC (MAR-1) (Invitrogen), CD117-eFluor 450 (2B8) (eBioscience). Ear total cellularity was determined using a Cellometer with AO/PI (Nexcelom), and dLN and spleen total cellularity was determined using a Z2 Coulter Particle Count and Size Analyzer (Beckman Coulter). Data was acquired on a LSR II flow cytometer (BD Biosciences) and analyzed using FlowJo v10 software (TreeStar Inc., Ashland, OR). Cellular populations were defined using the gating strategies outlined in **Supplemental Table 1**; Fluorescence minus ones (FMOs) were used as gating controls. An example of gating strategies for dLN, spleen, and ear is outlined in (Weatherly et al., 2024b).

2.8. Gene expression

Ear (half an ear pinna/mouse) and liver (caudate) were homogenized on a TissueLyser II in Buffer RLT (Qiagen). Total RNA was isolated using Qiagen's RNeasy mini spin column kits with DNase treatment on a QIAcube automated RNA isolation machine. RNA concentrations and purity were analyzed on a NanoDrop spectrophotometer (Thermo Fisher Scientific). The cDNA was prepared from 1 to 2 μg of RNA on an Eppendorf Mastercycler using Applied Biosystems' High-Capacity Reverse Transcription kit. The cDNA was used as a template for real-time PCR reactions containing TaqMan PCR Master Mix with gene-specific primers (Applied Biosystems) on a 7500 Real-Time PCR System. Relative fold gene expression changes ($2^{-\Delta\Delta CT}$) were determined compared to vehicle controls and normalized for expression of reference gene β-actin (Taqman). Evaluated genes are identified in Supplemental Table 2, and those with greater than a two-fold statistically significant change at any exposure were included in the results section.

2.9. Histology

Each tissue sample stored in 10 % formalin was embedded in paraffin, sectioned at 5 μm, stained with hematoxylin and eosin (H&E), and evaluated by a veterinary pathologist at StageBio (Mason, Ohio) using The Society of Toxicologic Pathology Guideline (Crissman et al., 2004). Provantis™ pathology software v10.2.3.1 was utilized for data capture and table generation. Histopathology grades were assigned as grade 1 (minimal), grade 2 (mild), grade 3 (moderate), grade 4 (marked), or grade 5 (severe) based on an increasing extent of change. The criteria used for skin grading were previously described (Weatherly et al., 2021).

2.10. Statistical analysis

A one-way analysis of variance (ANOVA) was conducted for analysis of the data generated from the described animal studies. If the ANOVA showed significance at $p \leq 0.05$, the Dunnett's Multiple Range *post*-test was used to compare treatment groups with the control group. No correction for multiple endpoints has been applied. Statistical analysis was performed using GraphPad Prism version 9.2 (San Diego, CA). Results represent the mean ± standard error (SE) of 4–5 mice per group. Statistical significance is designated by *p ≤ 0.05, **$p \leq 0.01$, and ***$p \leq 0.001$.

3. Results

3.1. PFBS and PFPeS increased serum and urine PFAS concentrations after 28-day dermal exposure

A significant increase in PFBS serum concentration was observed with 1.25, 2.5, and 5 % PFBS (Fig. 1A); levels increased from 0 μg/mL (control) to 4.3, 6.72, and 13.6 μg/mL, respectively. PFPeS levels in the serum were also significantly increased with 1.25, 2.5, and 5 % exposure, increasing from 0.766 μg/mL (control) to 41, 79.8, and 119.2 μg/mL, respectively (Fig. 1A), suggesting potential absorption occurring following PFAS dermal exposure. In general, serum PFPeS levels were higher than those for PFBS. Statistical analysis could not be performed on the urine samples as each concentration was from five pooled samples with a single data point. Urine PFBS concentration increased from 0 (control) to 72 μg/mL with 1.25 % PFBS, 250 μg/mL with 2.5 % PFBS, and 310 μg/mL with 5 % PFBS (Fig. 1B). Urine PFPeS concentration increased from 1.5 (control) to 220 μg/mL with 1.25 % PFPeS, 430 μg/mL with 2.5 % PFPeS, and 470 μg/mL with 5 % PFPeS (Fig. 1B). Notably, the longer-chain PFAS, PFPeS, had higher levels detected in the serum, but not in the urine.

3.2. Both PFBS and PFPeS dermal exposure for 28 days resulted in significantly altered organ weights

A significant increase in relative liver weights was observed with PFBS and PFPeS, along with a decrease in spleen weight with PFPeS exposure (Fig. 2). Relative liver weight significantly increased following exposure to 2.5 and 5 % PFBA and PFPeS (11, 14 %, and 32, 63 %, respectively, vs. values for vehicle-treated mice) (Fig. 2A). Relative spleen weights were significantly decreased by 18 % with the highest PFPeS (5 %) concentration (Fig. 2C). No change in relative weight was observed in the thymus or kidneys (Fig. 2B, D). No overt toxicity was observed with PFBS or PFPeS exposure, as measured in loss of body weight (Supplemental Fig. 1). Absolute organ weights not corrected for total body weight are reported in Supplemental Table 3, with significant increases only in liver mass with 1.25, 2.5, and 5 % PFPeS exposure. No significant changes in any absolute organ weights were observed with PFBS.

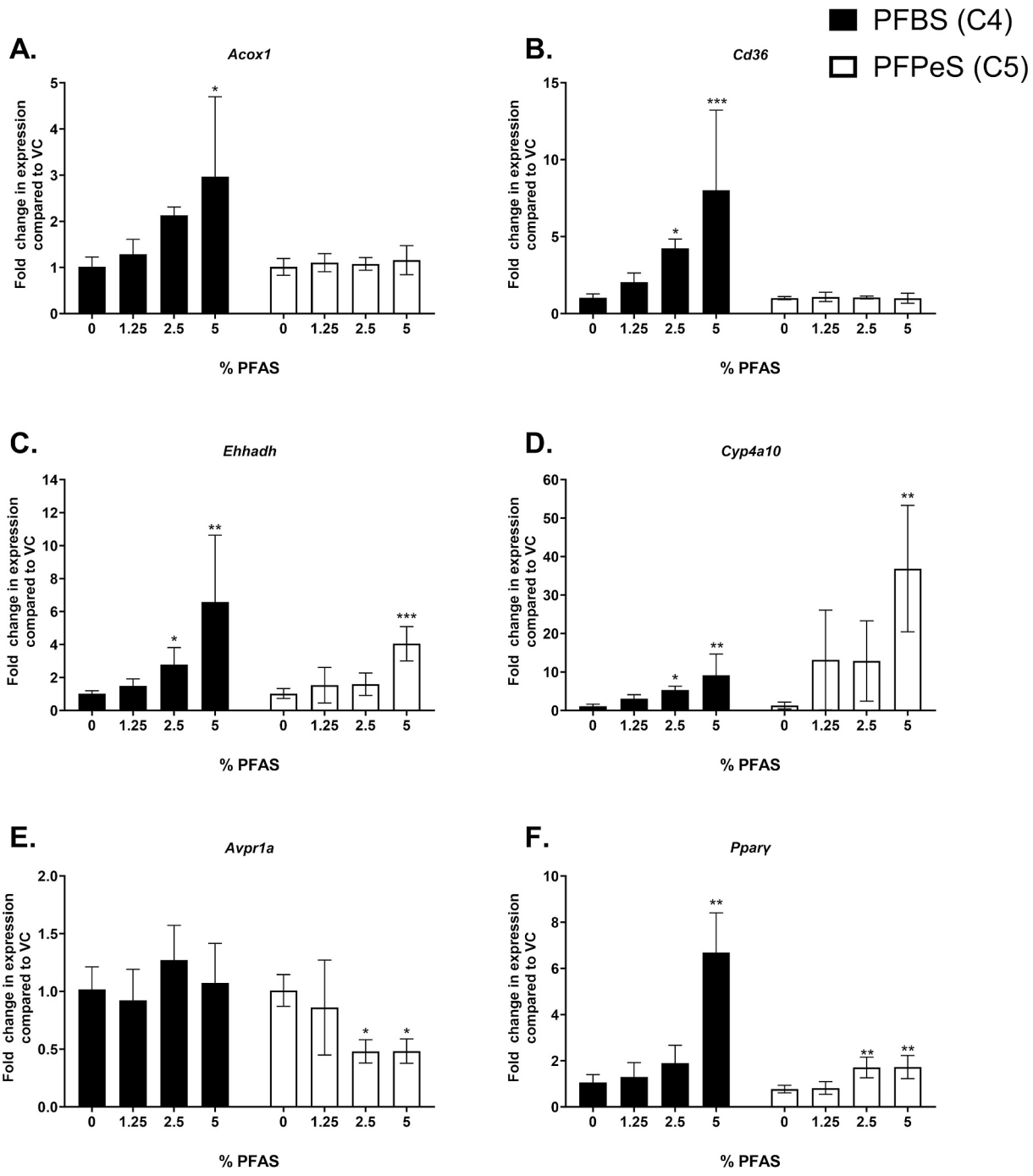

Fig. 4. Altered liver gene expression following 28 days of dermal exposure to PFBS or PFPeS. Changes in (A) *Acox1*, (B) *Cd36*, (C) *Ehhadh*, (D) *Cyp4a10*, (E) *Avpr1a*, and (F) *Pparγ* were evaluated. Data is shown as the mean (± SE) of 4–5 mice/group. Statistical significance, relative to 0% vehicle control (VC), was determined by one-way ANOVA with Dunnett's post-test, where *$p < 0.05$, **$p < 0.01$, ***$p < 0.001$.

3.3. Dermal exposure to PFBS or PFPeS alters serum chemistries

After 28 days of PFBS or PFPeS exposure, there was a significant increase in serum glucose (5 % PFBS; 1.25, 2.5, 5 % PFPeS) and alkaline phosphatase (ALKP) (5 % PFPeS) (Fig. 3A, B). Glucose increased following 5 % PFBS exposure by 25 % and by 28, 24, and 25 % with PFPeS exposure (1.25, 2.5, and 5 %, respectively) (Fig. 3B). ALKP increased 47 % but only following exposure to 5 % PFPeS (Fig. 3A). No significant changes were observed in cholesterol, ALT, or BUN (Fig. 3C-E).

3.4. Exposure to PFBS or PFPeS results in histopathological changes in the liver and skin

Histopathology examination of the liver revealed PFBS exposure induced minimal hepatocellular hypertrophy in all 5 % exposed animals (Table 1). Hepatocellular hypertrophy was characterized by decreased glycogen content, increased cytoplasmic eosinophilia, and increased hepatocyte volume predominantly in centrilobular locations. Similarly, but to a greater degree, PFPeS exposure induced minimal hepatocellular hypertrophy with 1.25 % (3/5 mice), mild hypertrophy in 1.25 % (1/5)

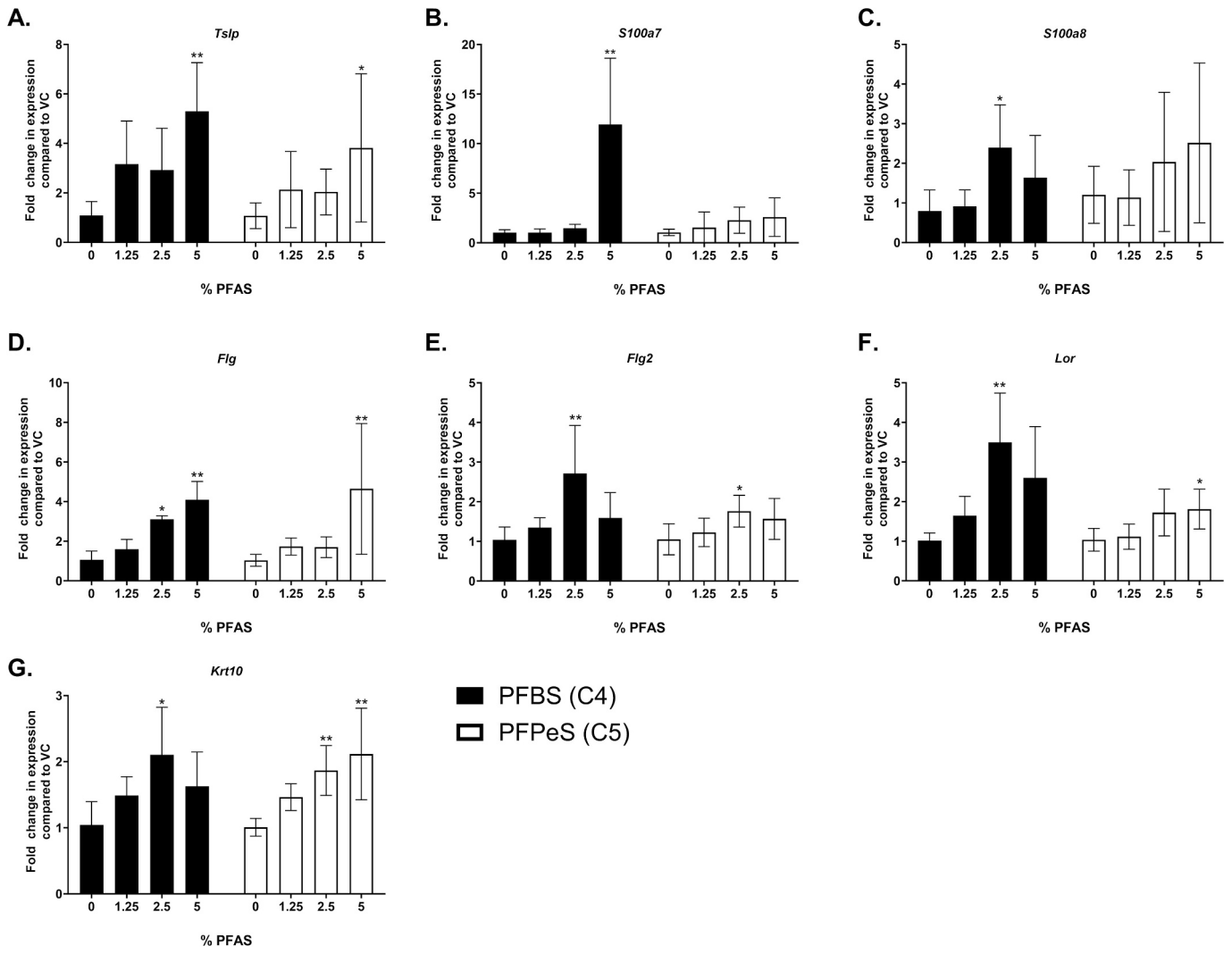

Fig. 5. Skin gene expression following 28 days of dermal exposure to PFBS or PFPeS. Changes in (A) *Tslp*, (B) *S100a7*, (C) *S100a8,* (D) *Flg*, (E) *Flg2,* (F) *Lor,* and (G) *Krt10* were evaluated. Data shown as the mean (± SE) of 4–5 mice/group. Statistical significance, relative to 0% vehicle control (VC), was determined by one-way ANOVA with Dunnett's post-test, where *p < 0.05, **p < 0.01.

Table 2
Skin phenotyping of mice dermally exposed to PFBS or PFPeS.

	28 days							
Skin	PFBS (C4) (v/v)				PFPeS (C5) (v/v)			
Parameter	0 %	1.25 %	2.5 %	5 %	0 %	1.25 %	2.5 %	5 %
Cellularity (x 10^6)	1.10 ± 0.16	1.32 ± 0.08	1.18 ± 0.09	1.11 ± 0.09	1.03 ± 0.07	1.01 ± 0.09	1.13 ± 0.06	1.17 ± 0.08
$CD45^+$ (x 10^4)	7.81 ± 0.95	10.10 ± 0.74	**11.80 ± 0.88***	**15.60 ± 0.17*****	11.00 ± 1.13	9.95 ± 1.39	11.60 ± 1.67	13.50 ± 0.14
$CD45^+$ (%)	7.21 ± 0.26	7.72 ± 0.53	**10.21 ± 0.85***	**14.04 ± 0.82*****	10.60 ± 0.46	9.67 ± 0.88	10.04 ± 1.07	11.43 ± 0.51
$CD4^+$ (x 10^3)	1.52 ± 0.19	2.34 ± 0.38	**3.50 ± 0.25****	**5.10 ± 0.58*****	1.87 ± 0.21	2.51 ± 0.45	2.83 ± 0.38	**4.62 ± 0.77****
$CD4^+$ (%)	1.96 ± 0.12	2.27 ± 0.23	**2.98 ± 0.19****	**3.28 ± 0.10*****	1.70 ± 0.10	2.43 ± 0.22	**2.51 ± 0.26***	**3.33 ± 0.23*****
$CD8^+$ (x 10^2)	1.16 ± 0.17	1.63 ± 0.41	1.88 ± 0.20	**2.39 ± 0.20***	2.97 ± 1.00	1.78 ± 0.14	1.89 ± 0.34	2.62 ± 0.47
$CD8^+$ (%)	0.16 ± 0.03	0.16 ± 0.03	0.16 ± 0.02	0.16 ± 0.01	0.26 ± 0.06	0.19 ± 0.02	0.16 ± 0.01	0.19 ± 0.02
NK (x 10^3)	1.93 ± 0.26	2.14 ± 0.34	**4.79 ± 0.45****	**5.40 ± 0.80*****	0.42 ± 0.04	0.38 ± 0.07	0.42 ± 0.06	0.76 ± 0.21
NK (%)	2.51 ± 0.29	2.06 ± 0.19	**4.06 ± 0.32****	3.46 ± 0.33	0.39 ± 0.04	0.37 ± 0.02	0.36 ± 0.02	0.55 ± 0.13
Eosinophils (x 10^3)	2.77 ± 0.64	3.49 ± 0.29	3.69 ± 0.24	**7.80 ± 0.86*****	2.21 ± 0.28	3.48 ± 0.54	3.56 ± 0.64	**7.21 ± 1.83****
Eosinophils (%)	3.60 ± 0.68	3.51 ± 0.36	3.15 ± 0.20	5.03 ± 0.37	2.03 ± 0.20	3.61 ± 0.40	3.03 ± 0.21	**4.96 ± 0.86****
Neutrophils (x 10^2)	8.59 ± 3.41	4.00 ± 0.58	3.12 ± 0.57	15.00 ± 4.90	10.90 ± 5.43	3.69 ± 0.80	15.80 ± 9.00	12.30 ± 3.91
Neutrophils (%)	1.05 ± 0.34	0.40 ± 0.06	**0.27 ± 0.05***	0.90 ± 0.23	1.14 ± 0.58	0.35 ± 0.04	1.10 ± 0.51	0.90 ± 0.28
Total DCs (x 10^3)	5.06 ± 0.52	6.92 ± 0.58	**9.21 ± 0.74***	**11.90 ± 1.42*****	7.90 ± 0.64	7.93 ± 1.29	9.07 ± 1.12	**13.10 ± 2.13***
Total DCs (%)	6.52 ± 0.30	6.81 ± 0.15	**7.78 ± 0.24****	**7.66 ± 0.22****	7.24 ± 0.17	7.80 ± 0.57	7.98 ± 0.38	**9.44 ± 0.64***

Values are expressed as the means (± SE) for each group ($n = 5$ mice/group).
*$p < 0.05$, **$p < 0.01$, ***$p < 0.001$.

Table 3
Spleen phenotyping of mice dermally exposed to PFBS or PFPeS.

	28 days							
Spleen	PFBS (C4) (v/v)				PFPeS (C5) (v/v)			
Parameter	0 %	1.25 %	2.5 %	5 %	0 %	1.25 %	2.5 %	5 %
Cellularity (x 10^8)	1.23 ± 0.03	1.36 ± 0.16	1.17 ± 0.04	1.19 ± 0.09	0.88 ± 0.04	0.87 ± 0.14	0.67 ± 0.06	0.55 ± 0.10
$CD4^+$ (x 10^7)	2.75 ± 0.09	2.97 ± 0.5	2.62 ± 0.13	2.68 ± 0.21	2.23 ± 0.08	1.92 ± 0.03	1.65 ± 0.15	**1.33 ± 0.23***
$CD4^+$ (%)	22.42 ± 0.58	21.60 ± 0.94	22.36 ± 0.82	22.42 ± 0.18	25.24 ± 0.49	22.82 ± 1.43	24.94 ± 1.08	24.22 ± 1.03
$CD8^+$ (x 10^6)	13.50 ± 1.48	16.10 ± 0.94	17.60 ± 2.42	16.40 ± 1.25	14.40 ± 0.61	12.10 ± 1.65	10.60 ± 1.00	**8.30 ± 1.44****
$CD8^+$ (%)	13.10 ± 0.45	12.84 ± 0.44	13.04 ± 0.75	13.76 ± 0.33	16.38 ± 0.64	14.24 ± 0.76	15.94 ± 0.70	15.12 ± 0.56
B-cells (x 10^7)	4.68 ± 0.13	5.22 ± 0.54	4.42 ± 0.16	4.38 ± 0.30	2.92 ± 0.16	3.23 ± 0.58	2.27 ± 0.27	1.96 ± 0.37
B-cells (%)	38.16 ± 0.73	38.56 ± 1.12	37.76 ± 0.86	36.80 ± 0.32	33.04 ± 0.85	36.36 ± 1.69	33.78 ± 1.83	35.30 ± 1.15
NK (x 10^5)	29.00 ± 4.26	23.80 ± 1.24	32.10 ± 3.65	26.70 ± 2.68	26.50 ± 1.33	27.10 ± 3.82	20.20 ± 3.15	**11.20 ± 1.46****
NK (%)	1.94 ± 0.08	**2.37 ± 0.07***	**2.61 ± 0.17****	2.22 ± 0.11	3.01 ± 0.11	3.17 ± 0.16	3.01 ± 0.37	2.16 ± 0.22
Neutrophils (x 10^5)	16.90 ± 1.56	14.50 ± 2.03	12.30 ± 1.98	15.00 ± 2.60	9.02 ± 0.83	6.98 ± 1.37	4.11 ± 0.47	4.12 ± 0.79
Neutrophils (%)	1.38 ± 0.12	1.07 ± 0.12	1.06 ± 0.18	1.24 ± 0.16	1.02 ± 0.08	0.79 ± 0.06	0.61 ± 0.02	0.75 ± 0.04
Dendritic Cells (x 10^6)	2.96 ± 0.33	2.65 ± 0.03	2.99 ± 0.50	2.59 ± 0.20	1.25 ± 0.07	1.35 ± 0.22	1.07 ± 0.11	0.87 ± 0.20
Dendritic Cells (%)	2.16 ± 0.04	2.16 ± 0.12	2.21 ± 0.10	2.18 ± 0.10	1.42 ± 0.06	1.56 ± 0.14	1.60 ± 0.05	1.56 ± 0.12
$CD11b^+$ (x 10^6)	5.59 ± 0.18	6.40 ± 0.73	5.82 ± 0.13	5.91 ± 0.71	2.72 ± 0.14	3.36 ± 0.55	2.30 ± 0.27	1.82 ± 0.37
$CD11b^+$ (%)	4.55 ± 0.10	4.70 ± 0.09	4.98 ± 0.10	4.90 ± 0.31	3.08 ± 0.11	**3.85 ± 0.15***	3.43 ± 0.22	3.29 ± 0.21

Values are expressed as the means (± SE) for each group (n = 5 mice/group).
*$p < 0.05$, **p < 0.01, ***p < 0.001.

and 2.5 % (5/5), and moderate hypertrophy with 5 % (5/5) (Table 1). With increasing severity, more of the hepatic plate was affected. Moderately affected individuals also had distortion of the hepatic cords surrounding the central vein. Individual animals dosed with 2.5 and 5 % PFPeS also had focal or multifocal randomly distributed necrosis of hepatocytes, which was likely related to hepatocellular hypertrophy. Minimal hepatocyte necrosis occurred in 3/5 mice in 2.5 % and 2/5 mice in 5 % PFPeS exposure groups. No necrosis was observed with PFBS exposure. No histopathological changes were observed in the liver with 0 % PFBS or PFPeS vehicle controls.

At the site of exposure, dose-related epidermal hyperplasia, or an increased number of keratinocyte layers, was observed with PFBS and PFPeS exposure. Minimal hyperplasia was observed at 1.25 % (1/5 mice), 2.5 % (3/5), and 5 % (5/5) PFBS and with 5 % PFPeS (5/5) (Table 1). Minimal mixed cell inflammation was also observed in the dermis with 2.5 % (1/5) and 5 % (2/5) PFBS and with 5 % (3/5) PFPeS exposure (Table 1). Mixed cell inflammation was characterized by neutrophils, lymphocytes, and/or macrophages scattered within the dermis subjacent to areas of epidermal hyperplasia. No histopathological changes were observed in the skin within any of the 0 % control groups (acetone). No biologically significant changes were identified in the spleen or kidney with exposure.

3.5. Dermal PFBS and PFPeS exposure results in changes in gene expression in the liver and skin

Select gene expression profiles in the liver were investigated based on gene profiling data generated from previous findings, summarized in Table 4 (Weatherly et al., 2024b). Most of the significant responses demonstrated a dose-dependent trend for both liver and skin. Genes with statistically significant differences in the liver that also exhibited greater than a 2-fold change in expression are shown in Fig. 4. Genes with statistically significant differences in the liver but less than a 2-fold change in expression are shown in Supplemental Fig. 2. Genes involved in steatosis (*Cd36*), fatty acid metabolism (*Acox1, Cyp4a10, Ehhadh*), hepatoxicity (*Avpr1a*), and PPAR ligand transport (*Cd36*) were significantly altered with either PFBS or PFPeS exposure (Fig. 4). Increases in *Acox1* (2.13 and 2.97-fold) and *Cd36* (4.24 and 8.00-fold) were unique to PFBS and observed with 2.5 and 5 % exposure respectively (Fig. 4A, B). PFBS (2.5 and 5 %) induced increases in *Ehhadh* (2.79 and 6.59-fold) and *Cyp4a10* (5.34 and 9.20-fold), and 5 % PFPeS increased *Ehhadh* 4.05-fold and *Cyp4a10* 36.87-fold (Fig. 4C, D). A decrease in *Avpr1a* was demonstrated with 2.5 and 5 % PFPeS (0.48 and 0.48-fold) (Fig. 4E); no change was observed following PFBS exposure. PPAR isoforms were also evaluated, with *Pparγ* expression increasing with 5 % PFBS and 2.5 and 5 % PFPeS exposure (Fig. 4F). Gene expression of *Apoa1*, *Cyp7a1, Pparδ*, and *Serpine1* was not altered in the livers with either PFBS or PFPeS exposure (data not shown).

The dermal toxicity was further evaluated with investigations of inflammatory responses and skin barrier integrity. In the skin, the danger signal, *Tslp*, increased with 5 % PFBS (5.30-fold) and PFPeS (3.82-fold) exposure (Fig. 5A). Expression of both danger-associated molecular patterns (DAMPs) *S100a7a* and *S1008a* significantly increased in the skin following PFBS exposure, with *S100a7a* having the largest increase (5 %; 11.92-fold) (Fig. 5B, C). Similar changes were observed with 4 skin barrier integrity genes following exposure to PFBS or PFPeS (Fig. 5). PFBS (2.5 and 5 %) and PFPeS (5 %) exposure increased *Flg* gene expression (Fig. 5D) while *Flg2* increased with 2.5 % PFBS and PFPeS (Fig. 5E). Gene expression of *Lor* and *Krt10* increased with 2.5 % PFBS, while PFPeS exposure significantly increased *Lor* with 2.5 % and *Krt10* with 2.5 % and 5 % (Fig. 5F, G). Gene expression of *Cxcl1, Il-1β, Il-6, Itgbl1, Krt14, Pparα, δ,* or *γ,* and *Serpine1* was not altered in the skin with either PFBS or PFPeS exposure (data not shown).

3.6. Dermal exposure of PFBS or PFPeS for 28 days results in significant phenotypic changes in the skin, dLN, and spleen

Phenotypic analysis of the ear pinna following 28 days of PFBS and PFPeS exposure showed alterations of several cellular sub-groups (Table 2). Interestingly, PFBS demonstrated more phenotypic changes in the ear compared to PFPeS. In the absence of increases in total cellularity, PFBS (2.5 and 5 %) exposure significantly increased cell number and frequency of $CD45^+$ cells, $CD4^+$ cells, natural killer cells (NK), and dendritic cells (DC). PFBS exposure also increased $CD8^+$ and eosinophil cell numbers but decreased neutrophil cell frequency (Table 2). PFPeS (5 %) only increased $CD4^+$, eosinophil, and DCs cell numbers and frequency (Table 2). The increased changes following PFBS were supported, in part, by the gene expression and histological evaluations.

Fewer changes were observed in the dLN and spleen. In the spleen, PFBS increased NK cell frequency (1.25 and 2.5 %) while PFPeS decreased $CD4^+$, $CD8^+$, and NK cell number (5 %) (Table 3). Although

Table 4
Comparison of liver changes following dermal exposure to sulfonic acid PFAS in mice.

	Liver Histology, Gene Expression, and Serum Chemistry						
	Weight	Histology	Gene Expression[#]	ALT	ALKP	BUN [*](kidney)	Reference
C4 (PFBS)	↑	Minimal hypertrophy	*Acox1, Cd36 Cyp4a10, Ehhadh, Lpl, Pparα, Pparγ*	NC	NC	NC	
C5 (PFPeS)	↑	Minimal to moderate hypertrophy, minimal necrosis	*Avpr1a↓, Cpt1b, Cyp4a10, Ehhadh, Pla2g12a, Pparα, Pparγ*	NC	↑	NC	
C6 (PFHxS)	↑	Marked hypertrophy, minimal to mild necrosis, inflammation	*Acox1, Apoa1↓, Avpr1a↓, Cd36, Cpt1b, Cyp4a10, Cyp7a1↓, Ehhadh, Lpl, Pla2g12a, Pparδ↓, Pparγ, Serpine1*	↑	↑	↓	Weatherly et al., 2024b
C7 (PFHpS)	↑	Mild to marked hypertrophy, minimal necrosis, inflammation	*Acox1, Apoa1↓, Avpr1a↓, Cd36, Cpt1b, Ctse, Cyp4a10, Ehhadh, Fabp1, Lpl, Pla2g12a, Pparδ↓, Serpine1*	↑	↑	NC	Weatherly et al., 2024a
C8 (PFOS)	↑	Moderate hypertrophy, minimal necrosis	*Acox1, Apoa1↓, Avpr1a↓, Cd36, Cpt1b, Ctse, Cyp4a10, Ehhadh, Fabp1, Lpl, Pla2g12a, Pparδ↓, Serpine1*	↑	↑	NC	Weatherly et al., 2024a

Note: No change (NC).
[*] No change in kidney weights for any compound evaluated.
[#] Gene expression is increased unless otherwise noted.

not reaching statistical significance, there was a decreasing trend in spleen cellularity following PFPeS exposure. In the dLN, PFBS increased $CD8^+$ cell numbers (2.5 %) and decreased eosinophil cell frequency (2.5 and 5 %) while PFPeS increased eosinophil cell number with only the 1.25 % exposure (Supplemental Table 4).

4. Discussion

High-quality scientific data to better understand PFAS exposure pathways and toxicological mechanisms to inform federal decisions that reduce risks to human health and the environment is needed (ITRC, 2023). Additionally, scientific interest and research efforts to identify PFAS alternatives or understudied PFAS and evaluate their effects on human health are growing. A wide range of chemical structures exist under the definition of PFAS, including precursor compounds that transform into varying PFAS. This provides opportunities to prioritize PFAS individually or by defined categories according to their chemical structure, physical-chemical properties, toxic effects, occurrence, use, or other characteristics.

This paper is the final in a series to investigate the systemic and immunotoxicity of representative sulfonic and carboxylic acid PFAS following dermal exposure in a murine model. The results presented in this manuscript report the findings for the sulfonic acids, PFPeS and PFBS. In general, the results were similar for the two compounds, as evidenced by liver weights, gene expression, pathology, spleen weights, and serum chemistries. These findings align with previous reports for the longer chain sulfonic acid PFAS (PFHxS, PFHpS, and PFOS) and suggest that systemic and immunotoxicity potential is linear in relation to carbon chain length for the tested sulfonic acids, Tables 4–7 (Weatherly et al., 2024a, 2024b). A hallmark of PFAS exposure in mice is increased liver weights. Exposure to both PFAS, PFBS or PFPeS, resulted in significant increases in liver weight. However, the increase in relative liver weight was larger for PFPeS-exposed mice compared to PFBS-exposed mice. Hepatic effects were also reinforced by changes in liver gene expression, histopathology, and elevated ALKP (PFPeS only), which also supported increased toxicity for the longer carbon-chain PFAS. While the general trends in liver gene expression were similar for the two PFAS, unique differences were identified. For example, while PFBS exposure resulted in increased expression of *Acox1* and *Cd36*, genes that have key roles in liver fatty acid metabolism and serum lipid abundance (Lu et al., 2024; Wilson et al., 2016), PFPeS exposure reduced expression of *Avpr1a,* a gene which may have a role in glucose metabolism (Yoshimura et al., 2021). However, when comparing these findings to the other sulfonic acids tested, these and other genes were altered following exposure to the longer-chain PFAS (C5-C8; Table 4), with a generally larger fold change with longer chain length.

In addition to the liver, the spleen was the only other organ demonstrating alterations in weight following exposure. While PFBS and PFPeS were not evaluated for immune function, exposure to the highest dose of PFPeS reduced spleen weights, suggesting potential immunotoxicity. PFPeS exposure also decreased $CD4^+$, $CD8^+$, and NK cell numbers in the spleen, but only at the highest concentration tested (Table 3). Although not reaching statistical significance, there was a decreasing trend in spleen cellularity also supporting the potential for immunotoxicity. No biologically significant spleen changes were observed for PFBS. The longer chain length sulfonic acid PFAS were all identified to be immunosuppressive, with their immunotoxicity also being linearly related to carbon chain length for the sulfonic acids (Table 5). Together, this suggests that sulfonic acid PFAS might target the adaptive immune system.

Similar to the other sulfonic acid PFAS that were investigated (Weatherly et al., 2024a, 2024b) (Table 6), PFBS and PFPeS were detected in the serum and urine following 28 days of exposure, with higher levels of PFPeS detected in the serum, suggesting a longer retention time or differing skin absorption rates based on carbon chain length. Exposure to 1.25 % for C4–7 PFAS compounds resulted in serum

Table 5
Comparison of immune outcomes of dermal exposure to sulfonic acid PFAS in mice.

Spleen Function, Pathology, and Phenotyping							
PFAS	Spleen Weights	Histology	Phenotyping	Response to SRBC immunization	NK cell activity	Thymus Weights	Reference
C4 (PFBS)	NC	NC	↑ % NK	ND	ND	NC	
C5 (PFPeS)	↓	NC	↓ # CD8, CD4, and NK	ND	ND	NC	
C6 (PFHxS)	↓	Mild decreased cellularity, lymphocyte	↓ # Total cells ↑ % CD8, CD4 ↓ % B-cells and NK cells ↑ % Neutrophils	↓	NC	↓	Weatherly et al., 2024b
C7 (PFHpS)	↓	Minimal decreased cellularity, lymphocyte	↓ # Total cells ↑ % CD8, CD4 ↓ # B-cells	↓	↑	↓	Weatherly et al., 2024a
C8 (PFOS)	↓*	Minimal decreased cellularity, lymphocyte	↓ # Total cells ↑ % CD8, CD4 ↓ #, % B-cells ↓ % DC	↓	↑	↓*	Weatherly et al., 2024a

Note: Sheep Red blood cells (SRBC); No change (NC); Not determined (ND).
* The weight of the organ is only significantly decreased by absolute weight not by % body weight.

Table 6
Comparison of metabolic changes and PFAS burden following dermal exposure to sulfonic acid PFAS in mice.

Metabolism and PFAS Burden					
	Cholesterol (mg/dL)	Glucose (mg/dL)	Serum (μg/mL) *	Urine (μg/mL) *	Reference
C4 (PFBS)	NC	↑	4.3	72	
C5 (PFPeS)	NC	↑	41	220	
C6 (PFHxS)	↓	↓	440	43	Weatherly et al., 2024b
C7 (PFHpS)	↑	↓	250	8.10	Weatherly et al., 2024a
C8 (PFOS)	↓	NC	145.6	0.82	Weatherly et al., 2024a

Note: No change (NC).
* Exposure concentration for serum and urine data is 1.25 % for C4-C7 compounds and 0.5 % for C8.

Table 7
Dermal changes following topical exposure to sulfonic acid PFAS in mice.

Skin Histology, Gene Expression, and Phenotyping					
	Histology	Inflammation Gene Expression*	Skin Integrity Gene Expression*	Phenotyping	Reference
C4 (PFBS)	Minimal hyperplasia and inflammation	*S100a7*, *S100a8*, *Tslp*	*Flg*, *Flg2*, *Krt10*, *Lor*	↑ % CD4 ↑ % NK	
C5 (PFPeS)	Minimal hyperplasia and inflammation	*Tslp*	*Flg*, *Flg2*, *Krt10*, *Lor*	↑ % CD4 ↑ % Eosinophils	
C6 (PFHxS)	NC	*Cxcl1*, *Il-6*, *Pparδ*, *Pparγ*↓, *S100a8*, *Serpine1*, *Tslp*	*Flg*, *Lor*	↑ % CD8 and CD4 ↓ % NK ↑ % Neutrophils	Weatherly et al., 2024b
C7 (PFHpS)	Minimal to mild hyperplasia	*Il-6*↓, *Pparα*↓, *Pparγ*, *Serpine1*, *Tslp*	*Flg*, *Itgb1*↓, *Krt10*↓, *Krt14*↓	↑ % CD8 ↓ % Eosinophils ↑ % Neutrophils	Weatherly et al., 2024a
C8 (PFOS)	NC	*Il-6*↓, *Pparα*↓, *Pparδ*	*Flg*↓, *Itgb1*↓, *Krt10*↓, *Krt14*↓	↑ % CD8 ↓ % NK	Weatherly et al., 2024a

Note: No change (NC).
* Gene expression is increased unless otherwise noted.

levels ranging from 4 to 440 μg/mL (Table 6). In general, the longer the sulfonic acid PFAS carbon chain, the lower the detection in the urine (72 μg/mL for PFBS versus 8 μg/mL for PFHpS), supporting a longer half-life and slower urinary elimination of the compound (Table 6). While potential oral exposure due to grooming and drinking water could not be avoided, these findings support the possibility of exposure via the skin.

The limited understanding of the dermal exposure route constitutes a serious knowledge gap, especially in light of the use of PFAS at relatively high concentrations in occupational settings and in consumer products that contact human skin for prolonged periods (Namazkar et al., 2024). Although studies are limited, exposure through the skin is supported by research conducted in our laboratory and by others (Chen et al., 2022; Ragnarsdóttir et al., 2023). Further considerations of factors affecting PFAS absorption, such as exposure conditions (dose, duration, surface area, exposure frequency), conditions of the skin surface (hydration, temperature, pH), and application sites, need consideration (Lin et al., 2023).

The molecular response in the skin for both PFAS was similar and included minimal hyperplasia and inflammation. Supporting the histological findings, changes in inflammatory genes, including *Tslp*, were observed. Similar to the liver, the inflammatory gene expression changes increased in number and fold change with increasing carbon chain length (Table 7). Changes in skin integrity genes were observed for all compounds, with *Flg* being altered for all tested PFAS (Table 7). The

phenotypic changes in the skin were minimal, with no obvious trends. While these findings support an impact on the skin, additional research is warranted.

There is an established relationship between PFAS exposure and metabolism; PFOA and PFOS have been reported to correlate with increased cholesterol levels in human serum (Dunder et al., 2022; Ragnarsdóttir et al., 2022). Interestingly, PFBS and PFPeS did not result in changes in cholesterol levels here; however, PFHxS and PFOS significantly decreased cholesterol, while PFHpS exposure resulted in increased levels (Table 6). Inconsistent trends were observed for the carboxylic acids tested as well; while PFBA increased cholesterol, consistent changes were not reported with PFPeA, PFHxA, or PFHpA exposure (Weatherly et al., 2021, 2023). Inconsistent trends were also observed for glucose levels (Table 6). Increased levels of glucose were reported for all carboxylic acids, while PFBS and PFPeS increased glucose, PFHxS and PFHpS decreased glucose, and no change was observed at the single concentration tested for PFOS (Weatherly et al., 2021, 2023). Several putative molecular initiating events for PFAS, in addition to nuclear receptor activation, include gap junctional inhibition to disrupt cell-cell communication, mitochondrial dysfunction, interference of protein binding, partitioning into lipid bilayers, oxidative stress, altered calcium homeostasis, and inappropriate activation of molecular signals controlling cell functions have been suggested; many of these effects are consistent with a nonspecific action of PFAS on the cellular lipid membrane (Bourre et al., 1989; Casares et al., 2019; Dodes Traian et al., 2012; Spector and Yorek, 1985). However, these events lack robust evidence to support a specific pathophysiological role in the multifaceted effects of PFAS. A better characterization of the modes of action or adverse outcome pathways (AOPs) for PFAS toxicities remains an important area of future investigation necessary to improve our understanding of PFAS impacts on human health (Liu et al., 2023).

A need for the characterization of common toxicological mechanisms and health effects resulting from PFAS exposure, including the potential classification of PFAS by toxicological mechanism and/or health effects, has been identified. While the liver was the only organ consistently affected by all PFAS tested (sulfonic acids and carboxylic acids; C4-C8), unique differences were identified between the two classes of PFAS. Particularly, immunotoxicity was linear for the sulfonic acids relating to chain length (Table 5) but was not observed for the carboxylic acids apart from PFOA. This may indicate different toxicological mechanisms between these classes of PFAS. However, differing toxicokinetic properties relating to functional group may also contribute to observed differences in toxicity. Exposure to sulfonic acid PFAS generally resulted in higher serum PFAS burdens relative to the serum burdens observed with carboxylic acid PFAS exposure (Weatherly et al., 2024a, 2024b; Weatherly et al., 2023). To illustrate, while exposure to the C4–7 sulfonic acid PFAS at 1.25 % resulted in serum PFAS concentrations from 4 to 440 μg/mL (Table 6), exposure to carboxylic acids PFPeA (C5) or PFHxA (C6) at 1.25 % resulted in average serum concentrations of 1.86 and 1.65 μg/mL (Weatherly et al., 2023). Additionally, the carboxylic acids were eliminated in the urine at higher concentrations than the sulfonic acids, also in a carbon chain length-associated manner (Weatherly et al., 2024a, 2024b; Weatherly et al., 2023). Exposure to the C5–7 sulfonic or carboxylic acid PFAS at 1.25 % resulted in urine sulfonic PFAS concentrations ranging from 8.10 to 220 μg/mL for the sulfonic acids (Table 6) and 340–3200 μg/mL for the carboxylic acids. Further work is needed to delineate the contributions of toxicokinetic properties versus molecular mechanisms in the health hazards associated with carboxylic vs sulfonic acid PFAS.

Due to the pervasive and persistent nature of these compounds, additional data is needed to better understand their potential acute and chronic health effects. Ultimately, the collective findings from these studies will help to address research gaps related to PFAS toxicity. While additional research is needed to underline the mechanisms of action, comparing skin absorption of different length and structure compounds is fundamental science that will help to inform discussion about assessment, prevent or minimize future exposure, and gain knowledge about toxicity.

Acknowledgements & funding

This work was supported by the National Occupational Research Agenda (NORA) CAN 9390HTP. This publication was additionally supported by a NIEHS-funded predoctoral fellowship to M.P.C. (T32ES032920). Its contents are solely the responsibility of the authors and do not represent the official views of the NIEHS or NIH.

The authors would like to thank Hillary L. Shane and Rachel Baur for their technical assistance. We would also like to acknowledge the online tool, BioRender, as it was used to construct the graphical abstract https://BioRender.com/2uw39br.

CRediT authorship contribution statement

Madison P. Cooper: Writing – review & editing, Writing – original draft, Visualization, Validation, Formal analysis, Data curation. **Lisa M. Weatherly:** Writing – review & editing, Writing – original draft, Visualization, Project administration, Investigation, Formal analysis, Conceptualization. **Ewa Lukomska:** Investigation. **Laurel G. Jackson:** Writing – review & editing. **Stacey E. Anderson:** Writing – review & editing, Writing – original draft, Supervision, Project administration, Investigation, Funding acquisition, Conceptualization.

Declaration of competing interest

The findings and conclusions in this report are those of the author(s) and do not necessarily represent the official position of the National Institute for Occupational Safety and Health (NIOSH), Centers for Disease Control and Prevention (CDC). Mention of any company or product does not constitute endorsement by NIOSH/CDC. The authors declare no conflicts of interest. The authors alone are responsible for the content of this manuscript.

Appendix A. Supplementary data

Supplementary data to this article can be found online at https://doi.org/10.1016/j.taap.2025.117487.

Data availability

The data of this study will be made available NIOSH Data and Statistics Gateway.

References

Alexander, B.H., Ryan, A., Church, T.R., Kim, H., Olsen, G.W., Logan, P.W., 2024. Mortality and cancer incidence in perfluorooctanesulfonyl fluoride production workers. Am. J. Ind. Med. 67 (4), 321–333. https://doi.org/10.1002/ajim.23568.

Andres, K.L., Olsen, G.W., Krisko, R.M., Nunnally, M.C., Boeding, R.R., Leniek, K.L., Taiwo, O.A., 2024. An investigation of 3M Cordova, IL production worker's per- and polyfluoroalkyl substances biomonitoring results and mortality experience. Int. J. Hyg. Environ. Health 256, 114321. https://doi.org/10.1016/j.ijheh.2024.114321.

Bourre, J.M., Francois, M., Youyou, A., Dumont, O., Piciotti, M., Pascal, G., Durand, G., 1989. The effects of dietary alpha-linolenic acid on the composition of nerve membranes, enzymatic activity, amplitude of electrophysiological parameters, resistance to poisons and performance of learning tasks in rats. J. Nutr. 119 (12), 1880–1892. https://doi.org/10.1093/jn/119.12.1880.

Casares, D., Escribá, P.V., Rosselló, C.A., 2019. Membrane lipid composition: effect on membrane and organelle structure, function and compartmentalization and therapeutic avenues. Int. J. Mol. Sci. 20 (9). https://doi.org/10.3390/ijms20092167.

Chen, Q., Yi, S., Ye, Q., Zhu, Y., Zhong, W., Zhu, L., 2022. Insights into the dermal absorption, deposition, and elimination of poly- and Perfluoroalkyl substances in rats: the importance of skin exposure. Environ. Sci. Technol. 56 (23), 16975–16984. https://doi.org/10.1021/acs.est.2c03181.

Crissman, J.W., Goodman, D.G., Hildebrandt, P.K., Maronpot, R.R., Prater, D.A., Riley, J. H., Seaman, W.J., Thake, D.C., 2004. Best practices guideline: toxicologic histopathology. Toxicol. Pathol. 32 (1), 126–131. https://doi.org/10.1080/01926230490268756.

Darrow, L.A., Groth, A.C., Winquist, A., Shin, H.M., Bartell, S.M., Steenland, K., 2016. Modeled Perfluorooctanoic acid (PFOA) exposure and liver function in a Mid-Ohio Valley community. Environ. Health Perspect. 124 (8), 1227–1233. https://doi.org/10.1289/ehp.1510391.

Dodes Traian, M.M., Cattoni, D.I., Levi, V., González Flecha, F.L., 2012. A two-stage model for lipid modulation of the activity of integral membrane proteins. PLoS One 7 (6), e39255. https://doi.org/10.1371/journal.pone.0039255.

Dunder, L., Lind, P.M., Salihovic, S., Stubleski, J., Karrman, A., Lind, L., 2022. Changes in plasma levels of per- and polyfluoroalkyl substances (PFAS) are associated with changes in plasma lipids - a longitudinal study over 10 years. Environ. Res. 211, 112903. https://doi.org/10.1016/j.envres.2022.112903.

Fairley, K.J., Purdy, R., Kearns, S., Anderson, S.E., Meade, B., 2007. Exposure to the immunosuppressant, perfluorooctanoic acid, enhances the murine IgE and airway hyperreactivity response to ovalbumin. Toxicol. Sci. 97 (2), 375–383. https://doi.org/10.1093/toxsci/kfm053.

Fenton, S.E., Ducatman, A., Boobis, A., DeWitt, J.C., Lau, C., Ng, C., Smith, J.S., Roberts, S.M., 2021. Per- and Polyfluoroalkyl substance toxicity and human health review: current state of knowledge and strategies for informing future research. Environ. Toxicol. Chem. 40 (3), 606–630. https://doi.org/10.1002/etc.4890.

Franko, J., Meade, B.J., Frasch, H.F., Barbero, A.M., Anderson, S.E., 2012. Dermal penetration potential of Perfluorooctanoic Acid (PFOA) in human and mouse skin. J. Toxicol. Environ. Health Part A 75, 50.

Gaines, L.G.T., Nylander-French, L.A., 2023. Occupational exposure to PFAS: research and protection needed. Am. J. Ind. Med. 66 (5), 424–426. https://doi.org/10.1002/ajim.23467.

Gluge, J., Scheringer, M., Cousins, I.T., DeWitt, J.C., Goldenman, G., Herzke, D., Lohmann, R., Ng, C.A., Trier, X., Wang, Z., 2020. An overview of the uses of per- and polyfluoroalkyl substances (PFAS). Environ Sci Process Impacts 22 (12), 2345–2373. https://doi.org/10.1039/d0em00291g.

Gomis, M.I., Vestergren, R., Borg, D., Cousins, I.T., 2018. Comparing the toxic potency in vivo of long-chain perfluoroalkyl acids and fluorinated alternatives. Environ. Int. 113, 1–9. https://doi.org/10.1016/j.envint.2018.01.011.

ITRC, 2023. PFAS Technical and Regulatory Guidance Document and Fact Sheets PFAS-1. Interstate Technology & Regulatory Council, PFAS Team. https://pfas-1.itrcweb.org.

Lin, X., Xing, Y., Chen, H., Zhou, Y., Zhang, X., Liu, P., Li, J., Lee, H.K., Huang, Z., 2023. Characteristic and health risk of per- and polyfluoroalkyl substances from cosmetics via dermal exposure. Environ. Pollut. 338, 122685. https://doi.org/10.1016/j.envpol.2023.122685.

Liu, S., Liu, Y., Zhang, D., Li, H., Shao, X., Xie, P., Li, J., 2023. Novel insights into perfluorinated compound-induced hepatotoxicity: chronic dietary restriction exacerbates the effects of PFBS on hepatic lipid metabolism in mice. Environ. Int. 181, 108274. https://doi.org/10.1016/j.envint.2023.108274.

Lu, D., He, A., Tan, M., Mrad, M., El Daibani, A., Hu, D., Liu, X., Kleiboeker, B., Che, T., Hsu, F.F., Bambouskova, M., Semenkovich, C.F., Lodhi, I.J., 2024. Liver ACOX1 regulates levels of circulating lipids that promote metabolic health through adipose remodeling. Nat. Commun. 15 (1), 4214. https://doi.org/10.1038/s41467-024-48471-2.

Lucas, K., Gaines, L.G.T., Paris-Davila, T., Nylander-French, L.A., 2023. Occupational exposure and serum levels of per- and polyfluoroalkyl substances (PFAS): a review. Am. J. Ind. Med. 66 (5), 379–392. https://doi.org/10.1002/ajim.23454.

McMahon, P.B., Tokranov, A.K., Bexfield, L.M., Lindsey, B.D., Johnson, T.D., Lombard, M.A., Watson, E., 2022. Perfluoroalkyl and Polyfluoroalkyl substances in groundwater used as a source of drinking water in the eastern United States. Environ. Sci. Technol. 56 (4), 2279–2288. https://doi.org/10.1021/acs.est.1c04795.

Namazkar, S., Ragnarsdottir, O., Josefsson, A., Branzell, F., Abel, S., Abou-Elwafa Abdallah, M., Harrad, S., Benskin, J.P., 2024. Characterization and dermal bioaccessibility of residual- and listed PFAS ingredients in cosmetic products. Environ Sci Process Impacts 26 (2), 259–268. https://doi.org/10.1039/d3em00461a.

NSTC PFAS Strategy Team, 2023. Per- and Polyfluoroalkyl Substances (PFAS) Report. Retrieved from. https://bidenwhitehouse.archives.gov/wp-content/uploads/2024/09/PFAS-STRAT-PLAN-FINAL.pdf.

NSTC PFAS Strategy Team, 2024. Per- and Polyfluoroalkyl Substances (PFAS) Federal Research and Development Strategic Plan. Retrieved from. https://bidenwhitehouse.archives.gov/wp-content/uploads/2024/09/PFAS-STRAT-PLAN-FINAL.pdf.

NTP, 2019. Toxicity studies of perfluoroalkyl carboxylates administered by gavage to Sprague Dawley (Hsd:Sprague Dawley SD) rats. Toxic Rep. Ser. 97. https://doi.org/10.22427/ntp-tox-97.

Panieri, E., Baralic, K., Djukic-Cosic, D., Buha Djordjevic, A., Saso, L., 2022. PFAS molecules: a major concern for the human health and the environment. Toxics 10 (2). https://doi.org/10.3390/toxics10020044.

Ragnarsdóttir, O., Abdallah, M.A.E., Harrad, S., 2022. Dermal uptake: an important pathway of human exposure to perfluoroalkyl substances? Environ. Pollut. 307, 119478.

Ragnarsdóttir, O., Abdallah, M.A., Harrad, S., 2023. Dermal bioaccessibility of perfluoroalkyl substances from household dust; influence of topically applied cosmetics. Environ. Res. 238 (Pt 1), 117093. https://doi.org/10.1016/j.envres.2023.117093.

Ragnarsdóttir, O., Abou-Elwafa Abdallah, M., Harrad, S., 2024. Dermal bioavailability of perfluoroalkyl substances using in vitro 3D human skin equivalent models. Environ. Int. 188, 108772. https://doi.org/10.1016/j.envint.2024.108772.

Shane, H.L., Baur, R., Lukomska, E., Weatherly, L., Anderson, S.E., 2020. Immunotoxicity and allergenic potential induced by topical application of perfluorooctanoic acid (PFOA) in a murine model. Food Chem. Toxicol. 136, 111114. https://doi.org/10.1016/j.fct.2020.111114.

Shoemaker, J.A., Grimmett, P., Boutin, B., 2008. Determination of Selected Perfluorinated Alkyl Acids in Drinking Water by Solid Phase Extraction and Liquid Chromatography/Tandem Mass Spectrometry (LC/MS/MS). DC Retrieved from, Washington. https://cfpub.epa.gov/si/si_public_record_report.cfm?Lab=NERL&dirEntryId=198984&simpleSearch=1&searchAll=EPA%2F600%2FR-08%2F092+.

Spector, A.A., Yorek, M.A., 1985. Membrane lipid composition and cellular function. J. Lipid Res. 26 (9), 1015–1035.

Steenland, K., Fletcher, T., Stein, C.R., Bartell, S.M., Darrow, L., Lopez-Espinosa, M.J., Barry Ryan, P., Savitz, D.A., 2020. Review: evolution of evidence on PFOA and health following the assessments of the C8 science panel. Environ. Int. 145, 106125. https://doi.org/10.1016/j.envint.2020.106125.

Tokranov, A.K., Ransom, K.M., Bexfield, L.M., Lindsey, B.D., Watson, E., Dupuy, D.I., Stackelberg, P.E., Fram, M.S., Voss, S.A., Kingsbury, J.A., Jurgens, B.C., Smalling, K.L., Bradley, P.M., 2024. Predictions of groundwater PFAS occurrence at drinking water supply depths in the United States. Science 386 (6723), 748–755. https://doi.org/10.1126/science.ado6638.

Trowbridge, J., Gerona, R.R., Lin, T., Rudel, R.A., Bessonneau, V., Buren, H., Morello-Frosch, R., 2020. Exposure to Perfluoroalkyl substances in a cohort of women firefighters and Office Workers in san Francisco. Environ. Sci. Technol. 54 (6), 3363–3374. https://doi.org/10.1021/acs.est.9b05490.

Wang, Z., Cousins, I.T., Scheringer, M., Hungerbühler, K., 2013. Fluorinated alternatives to long-chain perfluoroalkyl carboxylic acids (PFCAs), perfluoroalkane sulfonic acids (PFSAs) and their potential precursors. Environ. Int. 60, 242–248. https://doi.org/10.1016/j.envint.2013.08.021.

Weatherly, L.M., Shane, H.L., Lukomska, E., Baur, R., Anderson, S.E., 2021. Systemic toxicity induced by topical application of heptafluorobutyric acid (PFBA) in a murine model. Food Chem. Toxicol. 156, 112528. https://doi.org/10.1016/j.fct.2021.112528.

Weatherly, L.M., Shane, H.L., Lukomska, E., Baur, R., Anderson, S.E., 2023. Systemic toxicity induced by topical application of perfluoroheptanoic acid (PFHpA), perfluorohexanoic acid (PFHxA), and perfluoropentanoic acid (PFPeA) in a murine model. Food Chem. Toxicol. 171, 113515. https://doi.org/10.1016/j.fct.2022.113515.

Weatherly, L.M., Shane, H.L., Jackson, L.G., Lukomska, E., Baur, R., Cooper, M.P., Anderson, S.E., 2024a. Systemic and immunotoxicity induced by topical application of perfluoroheptane sulfonic acid (PFHpS) or perfluorooctane sulfonic acid (PFOS) in a murine model. J. Immunotoxicol. 21 (1), 2371868. https://doi.org/10.1080/1547691x.2024.2371868.

Weatherly, L.M., Shane, H.L., Jackson, L.G., Lukomska, E., Baur, R., Cooper, M.P., Anderson, S.E., 2024b. Systemic and immunotoxicity induced by topical application of perfluorohexane sulfonic acid (PFHxS) in a murine model. Food Chem. Toxicol. 186, 114578. https://doi.org/10.1016/j.fct.2024.114578.

Wilson, C.G., Tran, J.L., Erion, D.M., Vera, N.B., Febbraio, M., Weiss, E.J., 2016. Hepatocyte-specific disruption of CD36 attenuates fatty liver and improves insulin sensitivity in HFD-fed mice. Endocrinology 157 (2), 570–585. https://doi.org/10.1210/en.2015-1866.

Wu, N., Cai, D., Guo, M., Li, M., Li, X., 2019. Per- and polyfluorinated compounds in saleswomen's urine linked to indoor dust in clothing shops. Sci. Total Environ. 667, 594–600. https://doi.org/10.1016/j.scitotenv.2019.02.287.

Yoshimura, M., Conway-Campbell, B., Ueta, Y., 2021. Arginine vasopressin: direct and indirect action on metabolism. Peptides 142, 170555. https://doi.org/10.1016/j.peptides.2021.170555.

Zahm, S., Bonde, J.P., Chiu, W.A., Hoppin, J., Kanno, J., Abdallah, M., Blystone, C.R., Calkins, M.M., Dong, G.-H., Dorman, D.C., Fry, R., Guo, H., Haug, L.S., Hofmann, J.N., Iwasaki, M., Machala, M., Mancini, F.R., Maria-Engler, S.S., Møller, P., Schubauer-Berigan, M.K., 2024. Carcinogenicity of perfluorooctanoic acid and perfluorooctanesulfonic acid. Lancet Oncol. https://doi.org/10.1016/S1470-2045(23)00622-8.